



## Research Article

# Molecular dockings of secondary metabolites to evaluate anthelmintic potential

Dilara KARAMAN<sup>1,\*</sup>, Oya GİRİŞGİN<sup>2</sup>, Ahmet Onur GİRİŞGİN<sup>3</sup>

<sup>1</sup>Department of Bioengineering, Yildiz Technical University, İstanbul, 34220, Türkiye

<sup>2</sup>Karacabey Vocational School, Bursa Uludag University, Bursa, 16700, Türkiye

<sup>3</sup>Department of Parasitology, Veterinary Faculty, Bursa Uludag University, Bursa, 16059, Türkiye

## ARTICLE INFO

### Article history

Received: 18 September 2024

Revised: 02 December 2024

Accepted: 05 February 2025

### Keywords:

Anthelmintic; Artemisia; In Silico Docking; Momordica; Origanum

## ABSTRACT

Helminthic infection is an important health problem that affects millions of humans and animals, especially in developing countries. This study aims to research some natural compounds which can be used continuously in the treatment of recurrent helminthic infections. For this purpose, we predicted the anthelmintic properties of some bioactive compounds from *Artemisia annua* L., *Momordica charantia* L., *Origanum vulgare* subsp. *hirtum*, and *Rubus catescens* DC. These compounds were docked with anthelmintic target proteins; Hc $\beta$ -tubulin (*Haemonchus contortus*  $\beta$ -tubulin), AsFR (*Ascaris suum* fumarate reductase), and CPT 2 (rat carnitine palmitoyl transferase 2) enzyme using AutoDock 4.2 program. The chemical interactions and ADME properties of the most potent ligands were investigated via Biovia Discovery Studio Client 2020 and SwissADME. In the results, it was demonstrated, based on molecular interactions, that oreganol, momordicin II, cucurbitacin-B, and charantadiol-A have multi-inhibitory properties against target proteins. It was revealed for the first time that oreganol, cucurbitacin-B, charantadiol-A, and momordicin II inhibited CPT 2 and AsFR enzymes at nanomolar inhibition constants (0,137 nM, 0,0571 nM, 2,06 nM, and 0,072 nM for CPT 2 enzyme; 1,9 nM, 5,31 nM, 16,6 nM, and 40,78 nM for AsFR, respectively). Oreganol has also inhibited Hc $\beta$ -tubulin at low  $K_i$  values ( $K_i = 24,32$  nM). These findings hold significant implications in the medical field, as they indicate that the compounds in question could serve as broad-spectrum anthelmintic drugs. When broad-spectrum drugs are needed, the oreganol scaffold can be used since it is triple-acting inhibitor. Cucurbitacin-B can be a candidate molecule to replace Ivermectin because they compete for the same target. According to the study's findings, future anthelmintics may be developed from cucurbitacins, adding to the effective treatments already provided by benzimidazoles and macrocyclic lactones. This research represents the first instance in which essential *in silico* scientific data has been gathered to support this conclusion.

**Cite this article as:** Karaman D, Girişgin O, Girişgin AO. Molecular dockings of secondary metabolites to evaluate anthelmintic potential. Sigma J Eng Nat Sci 2026;44(1):575–591.

### \*Corresponding author.

\*E-mail address: [dilara.karaman@yahoo.com](mailto:dilara.karaman@yahoo.com)

This paper was recommended for publication in revised form by Editor-in-Chief Ahmet Selim Dalkilic



## INTRODUCTION

Helminthic infections are prevalent in almost all countries; however, they are more common in South America, Africa, and Asia. According to WHO data, 1.5 billion people around the world are infected with soil-transmitted helminths. Specifically, 819 million people have *Ascaris*, 464 million people have *Trichuris*, and 438 million people are infected with hookworm. Schistosomiasis is considered an epidemic disease in 83 countries, with an estimated 180 million cases predicted [1]. In addition to this, substantial expenses have been incurred for the prevention and treatment of helminthic infections in animals. Novel simulations are necessary to control helminthic diseases. A new technique that allows continuous visualization of the spread of the disease in different age groups was developed for Covid-19 control [2]. With this new simulation called Hybrid NAR-RBFs Networks, parameters were evaluated to see the effect of an infective disease in a very wide geography.

In regions with limited health services, people often face recurring helminthic infections and drug resistance issues. Exploring natural compounds as alternatives to synthetic drugs is crucial, but obtaining and studying these compounds can be costly and arduous. *In silico* molecular modelling, simulations play a key role in providing insights into potential drug interactions, serving as an important step in rational drug design. Protein-ligand docking simulation is also essential in reducing the cost and labor involved in drug research [3]. *In silico* modelling studies, which are the first step of drug discovery, should be increased because simulations created with chemical calculations at the atomic level serve as an aid in predicting the biological effect of the drug.

In drug research, *in silico* simulations, the first and probably the most important step, help to estimate the pharmacokinetics, pharmacodynamics and side effects of the drug. Pharmacokinetics consists of stages that involve reaching the target cell, which can be predicted through computational methods. These stages are related to the chemical and biological properties of a drug candidate. Pharmacokinetics is mainly concerned with ADMET (Absorption, Metabolism, Excretion, and Toxicity), which includes the absorption of the drug from the intestines, skin, and cell membranes, distribution in the body (including its reach to different cells, tissues, and organs, and whether it can penetrate the blood-brain barrier), the by-products formed as a result of metabolism (including its susceptibility to liver enzymes), excretion, and potential toxicities [4]. However, research methods related to ADME have been developed using computer programs to provide data on the absorption and distribution of the drug [5].

According to literature, the development of resistance to anthelmintics is inevitable [6]. Therefore, it is imperative to discover new and effective natural anthelmintic compounds as drug candidates. Hundreds of millions of people need anthelmintic drugs, but they cannot use them due to two important reasons: 1) Health problems (kidney failure,

liver problems, hair loss, etc.) resulting from frequent use of synthetic drugs in the treatment of frequent recurring helminthic infections; 2) The problem of access to local services for communities living in regions where health facilities are not sufficient [1]. Considering this situation, scientists who are responsible for developing drugs against helminthic infections need to provide scientific data on anthelmintic plants and their effectiveness, especially those that can grow in arid or tropical climates.

There are different target proteins being used for anthelmintic purposes. Beta-tubulin protein, being responsible for microtubulin formation and cell division, is a known target of benzimidazole class drugs such as Albendazole or Mebendazole. Fumarate reductase is considered as a target of Thiabendazole [7]. Carnitine palmitoyl transferase 2 (CPT 2) is a “chokepoint” enzyme for nematode survival. A CPT 2 inhibitor was demonstrated as an anthelmintic because of killing some hazardous nematodes such as *Haemonchus contortus* and *Onchocerca linealis* [8].

In this study, it was aimed to investigate four plants (*Artemisia annua* L., *Rubus canescens* DC., *Momordica charantia* L., and *Origanum vulgare* subsp. *hirtum*), which are species that can grow in a wide geography in the world, from an anthelmintic perspective using *in silico* methods. Bioactive compounds found in these plants were investigated by *in silico* dockings for the inhibition of three proteins (*Haemonchus contortus*  $\beta$ -tubulin protein (Hc $\beta$ -tubulin), *Ascaris suum* fumarate reductase (AsFR) enzyme and rat carnitine palmitoyl transferase 2 (CPT 2) enzyme), which are the potential targets of anthelmintics.

Since millions of mebendazole tablets are donated each year, resistance development may be seen in the near future [9]. This study showed which herbal components could be useful in the scaffold selection of new anthelmintics to be designed in case of resistance development and when broad-spectrum drugs are needed. Hc $\beta$ -tubulin was chosen as a target protein to investigate the alternative drugs to benzimidazoles. Three different target proteins were used to determine the broad-spectrum ability of novel herbal drug candidates.

In the treatment of river blindness, the only drug option is Ivermectin [10]. The use of Ivermectin in severe infections causes extremely itchy allergic reactions called Mazzotti reactions, which makes treatment difficult. Ivermectin is not licensed for use in humans. The use of this drug in humans is due to desperation, and this is a health problem that needs to be solved urgently. In this study, natural compounds that may be as effective as Ivermectin were investigated for the first time with computational tools.

## MATERIALS AND METHODS

### Preparation of Ligands

Fifty herbal ligands were chosen from four plants (*Artemisia annua* L., *Origanum vulgare* subsp. *hirtum*,

*Momordica charantia* L., and *Rubus canescens* DC). These herbal ligands were used in docking experiments (Figures, names, molecular formulas and PubChem IDs of these ligands were presented in Appendixes-1). Some of these components were downloaded from the PubChem database in sdf format and from the Zinc Database in mol2 format, while others were drawn and optimized with Biovia Discovery Studio Client 2020 (Biovia DS) [11]. Molecules in sdf format were converted to pdbqt format with Openbabel program, while others were converted into pdbqt with AutoDock Tool [12, 13].

### Preparation of Proteins

Biovia DS and Autodock 4.2 software were used for the preparation of the proteins. Proteins and enzymes that are drug targets in nematodes were investigated. Those target proteins and enzymes found in nematodes were downloaded from the Brookhaven Protein Databank (<http://www.rcsb.org/pdb>). These proteins are: *Ascaris suum* fumarate reductase enzyme PDB ID: 4YSX (mitochondrial rhodoquinol-fumarate reductase, solubility: 2.25 Å, bound with NN23 inhibitor [14]; *Haemonchus contortus*  $\beta$ -tubulin protein PDB ID: 1OJ0 (in complex with ABZ, theoretical structure) [15]; anthelmintic drug target rat carnitine o-palmitoyltransferase PDB ID: 2H4T (resolution: 1.90 Å, bound with dodecane (C<sub>12</sub>H<sub>26</sub>) [16] and PDB ID: 2FW3 (resolution: 2.50 Å) [17] seen as an important “chokepoint enzyme” in the literature. In determining target proteins, a study of Taylor et al. was referenced [7]. The ions and ligands and water molecules other than the cofactor were deleted. Missing hydrogen atoms were added. The missing atoms and bonds in the protein residues were manually checked for completion. After all the hydrogens were added, it was optimized first with the “Clean Geometry” tool and then with Charm forcefield by using Biovia DS program.

### Investigation of Adme Properties

SwissADME web server [5] was used to evaluate the absorption, metabolism, and excretion (ADME) properties of drug candidates. Via the SwissADME program, the gastrointestinal (GI) absorption, ability to penetrate the blood-brain barrier, and their interactions with important biological systems (such as P-gp, CYP1A2, CYP2C9, CYP2C19) were predicted with computational methods.

### Molecular Docking Experiment

In this study, it was planned to do docking experiments at different stages for different purposes.

Stage 1 - Preparation of Proteins: Re-docking procedure was applied during the preparation of crystallized proteins after they were taken from PDB. For this purpose, the natural ligand and water molecules of the protein were deleted and docked with its natural ligand after it was prepared, the parameters were changed and the re-docking process was repeated until the appropriate value was reached as a result of RMSD calculation.

Stage 2 - Docking of target proteins and herbal ligands: Some compounds that had been demonstrated in these plants scientifically in the previous research are docked with drug target proteins that have passed the first stage. For comparison, the same target proteins were also subjected to docking simulation with the drug molecules such as Albendazole (ABZ), Mebendazole (MBZ), Ivermectin (IVC), Piperazine and Praziquantel (PZQ). Since the PZQ is also anticestodal and antitrepatodal, it was investigated from an antinematodal perspective in this study.

The docking procedure is briefly as follows:

Selected ligands were docked using AutoDock 4.2 program with the proteins obtained from Protein Data Bank. Gridbox size was determined by the size of the ligand. The reactive atom of the cofactor in the protein was chosen as the center, or, in case it did not carry the cofactor, the natural ligand in the protein was taken to the Gridbox center. The atoms in the active region of the protein are released in motion, while other parts are kept rigid. In the docking process of proteins bound by their natural ligands in their co-crystalline forms, their natural ligands were taken as reference for RMSD calculations. The ionic strength was set to be 0.145 and the dielectric constant to 10. Docking analysis was performed with Lamarckian Genetic Algorithm 4.2 [18]. Using AutoDock 4.2 scoring functions, 10 or 20 runs were chosen for each ligand. After ranking according to their free binding energy, the highest-scoring ligands were analyzed in terms of their interactions at the binding site by AutoDock Tools and Biovia DS.

## RESULTS AND DISCUSSION

Docking results of small molecules showed several score values according to Table 1. Although some of these molecules (carvacrol, thymol, ellagic acid and piperazine) are anthelmintic, docking scores showed that their affinities to these three proteins (CPT 2 (pdb ID: 2H4T), AsFR (pdb ID: 4YSX), and Hc $\beta$ -tubulin (Pdb ID: 1OJ0)) were low because these molecules did not make enough number of interactions in terms of formulations which used in the calculation of free energy of binding. Also, another cause is probable that these molecules can bind to other receptors or proteins while the anthelmintic effect is performing.

It is known that MBZ inhibits the  $\beta$ -tubulin in helminths. In this study, Hc $\beta$ -tubulin inhibition of MBZ was found at 1 nM level, and this result was appropriate with the known anthelmintic effect of MBZ. It was found that it had a good affinity to the other two proteins (4,6 nM and 96,25 nM inhibition constant ( $K_i$ ) for CPT 2 and AsFR, respectively) ( $K_i$  values were presented in Appendixes-2).

A herbal ligand, oreganol, possessed the highest score with a 1,9 nM  $K_i$  value for AsFR enzyme (Fig. 2). Oreganol is a potential inhibitor for both the CPT2 enzyme and the AsFR. Based on these findings, oreganol is a promising candidate for an anthelmintic drug, marking the first instance of this bioactive molecule being investigated as an anthelmintic.

**Table 1.** Free binding energy of herbal ligands and drugs with protein targets

Molecule	1OJ0 $\Delta G$ (kcal/mol)	2H4T $\Delta G$ (kcal/mol)	4YSX $\Delta G$ (kcal/mol)
ABZ	-9.07	-6.87	-5.53
Ivermectin	1.25E+03	-13.01	8.98
MBZ	-12.23	-11.37	-9.57
Piperazine	-4.92	-5.11	-5.84
Praziquantel	-4.15	-10.06	-8.53
Charantadiol-A	18.06	-11.85	-10.61
Momordicin I	26.17	-10.83	-7.78
Momordicin II	72.67	-13.83	-10.08
Kuguacin-J	14.54	-11.04	-7.89
Karavilagenin-D	21.91	-10.99	-9.35
Cucurbitacin-B	17.9	-13.97	-11.29
$\alpha$ -Pinene	-6.34	-6.12	-4.67
$\alpha$ -Terpinene	-6.8	-5.98	-4.76
$\alpha$ -Thujene	-6.62	-6.09	-5.55
$\beta$ -Caryophyllene	-8.27	-8.08	-6.12
$\gamma$ -Terpinene	-6.8	-5.96	-4.83
Myrcene	-6.06	-5.45	-4.16
Borneol	-6.58	-6.83	-5.15
Terpinen-4-ol	-7.06	-6.67	-5.54
<i>p</i> -Cymen	-6.04	-5.28	-4.07
Thymol	-6.25	-5.55	-4.58
Carvacrol	-6.34	-5.64	-4.53
Diosmetin	-10.24	-10.77	-9.62
Apigenin	-10.75	-10.15	-8.78
Oreganol	-10.39	-13.45	-11.9
Eriodictyol	-9.58	-10.76	-9.42
Eriocitrin	+15.66	-8.43	-6.62
Linalool	-6.89	-6.65	-5.34
Luteolin	-9.85	-10.43	-9.27
Chrysoeriol	-10.21	-10.81	-8.83
Artemisinin	-7.09	-8.99	-6.45
Artemetin	-1.16	-6.78	-6.03
Artemisinic acid	-7.01	-7.17	-6.25
Deoxy artemisinin	-7.57	-8.62	-5.98
Friedelin	72.37	-10.76	-8.04
Arteannuin B	-10.68	-9.23	-7.82
Stigmasterol	5.17	-10.95	-8.42
Scopoletin	-9.28	-8.21	-7.23
Quersetin	-5.23	-6.92	-5.97
Camphene	-6.11	-6.15	-4.77
Camphor	-6.25	-6.62	-4.91
Chrysofenetin	-7.25	-10.58	-9.3
Chrysofenol-D	-7.15	-10.39	-9.18
Eucalyptol	-6.56	-6.54	-5.1
Isofraxidin	-10.21	-8.58	-7.03
Sabinene	-6.66	-6.13	-4.79
Scoparone	-9.4	-7.95	-7.15
Spathulenol	-8.33	-9.05	-6.58
Umckalin	-9.7	-8.49	-7.64
Diisooctyl phthalate	-7.56	-8	-6.91
Furan-2-carboxaldehyde	-6.18	-6.26	-6.93
Hexadecanoic acid methyl ester (methyl palmitate)	-6.63	-5.69	-3.92
9,12,15-octadecantrienoic acid methyl ester (ODTAME)	-10.54	-7.98	-6.19
Ellagic acid	-1.14	-7.11	-5.94
Gallic acid	-4.21	-5.25	-3.75

1OJ0: Hc $\beta$ -tubulin; 2H4T: CPT 2 enzyme; 4YSX: AsFR enzyme.

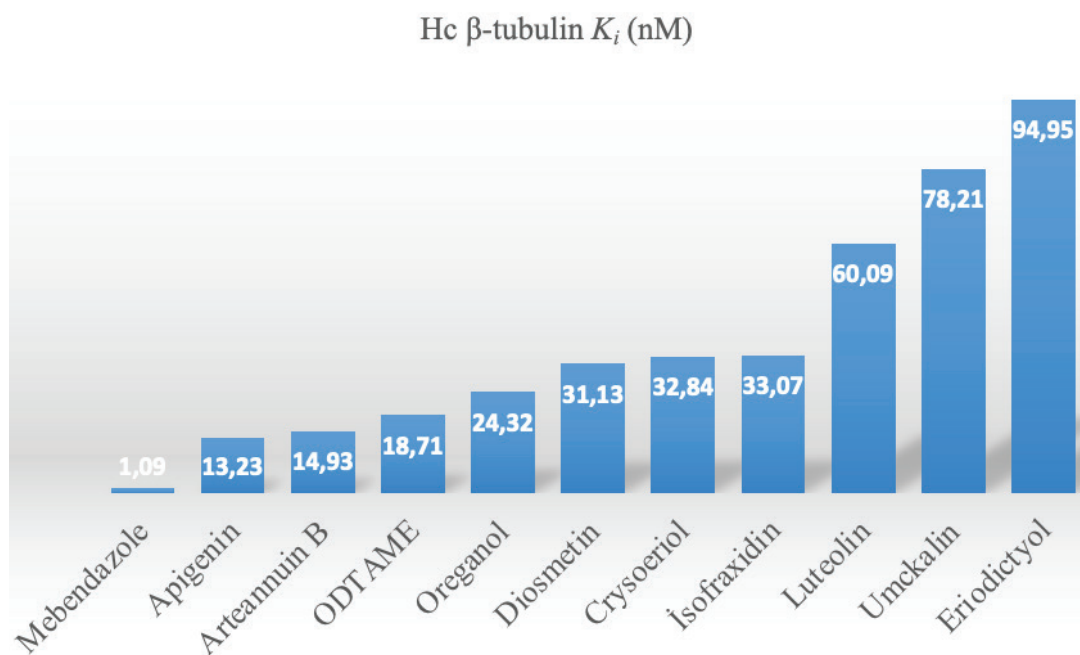


**Figure 1.** The first eleven molecules have the lowest  $K_i$  values against *H. contortus*  $\beta$ -tubulin (Hc $\beta$ -tubulin, pdb ID: 1OJ0).

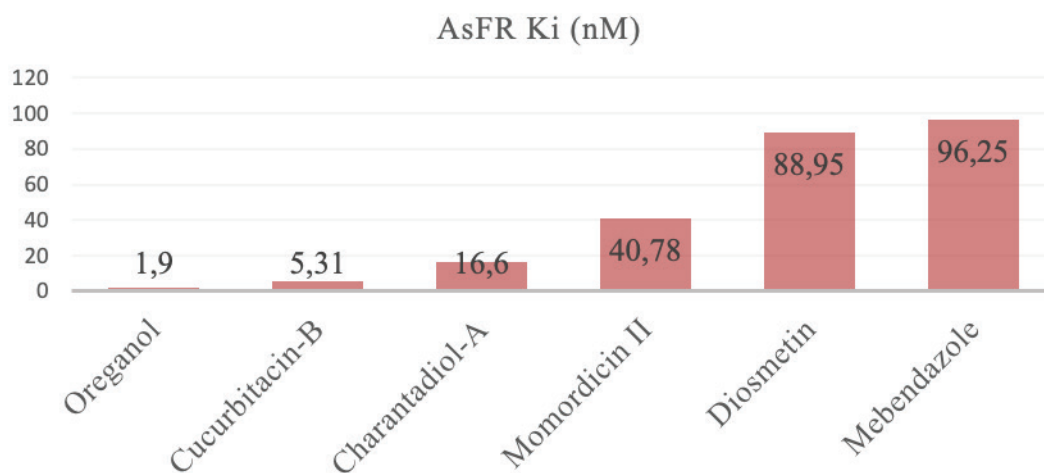


**Figure 2.**  $K_i$  values of best six molecules for AsFR (pdb ID: 4YSX).

The results in Table 1 show that IVC is antinematodal also *in silico*. Significantly, IVC was found to have a very good affinity to CPT 2 enzyme with the 290 pM  $K_i$  value. Since it was known that the rat CPT 2 enzyme is a target enzyme for *Onchocerca linealis* [19] and IVC is the only drug in the treatment of *Onchocerca volvulus* infection, this result has been showing that *in silico* experiments in this study provided the important data.

Although ABZ and MBZ are similar benzimidazole derivatives, the affinity of ABZ to CPT 2 and AsFR enzymes was found to be different from the MBZ's. While

Hc $\beta$ -tubulin inhibition of ABZ was found at a nanomolar level as expected, 9  $\mu$ M and 87,7  $\mu$ M  $K_i$  were observed against CPT 2 and AsFR enzymes, respectively. This result showed that ABZ inhibited the nematode's Hc $\beta$ -tubulin. Apparently, it could bind to two other target enzymes (CPT 2 and AsFR), too. PZQ is used as an antitrepatodal and anticestodal drug. These docking results showed that PZQ would also be able to be tried as an antinematodal in future *in vivo* experiments. Piperazin is a GABA agonist, so it cannot inhibit these enzymes (AsFR, CPT 2 or  $\beta$ -tubulin) in normal biological conditions. In this study, the results have

shown the correctness of the docking procedure, and they are correlated to the known anthelmintic effect of these synthetic drugs.

According to the results of AutoDock4.2, cucurbitacin-B, momordicin II, and oreganol inhibit the rat CPT 2 at picomolar (pM) levels. Cucurbitacin-B possessed very good  $K_i$  values, such as 57,11 pM against CPT 2 enzyme (pdb ID: 2H4T). 57, 11 pM is a very rare result, and it shows that this molecule has very significant anthelmintic potential. This result shows that it has discovered a novel and more effective drug candidate via computational methods in treating *Onchocerca volvulus* infection, which exists only a single drug option. Because it was not discovered hitherto via *in silico* methods, this study is the first study demonstrating with the docking simulations that cucurbitacin-B is an anthelmintic.

According to Figure 3, six molecules above 5 nM possess the best  $K_i$  values for CPT 2 enzyme inhibition. Two of them are IVC and MBZ, which were used commonly and marked as synthetic drugs. Cucurbitacin-B, momordicin II, oreganol, and charantadiol-A, which were found *in silico* as the best four anthelmintic ligands, are bioactive molecules obtained from *O. vulgare* subsp. *hirtum* and *M. charantia*. These results show that these herbal ligands will be more effective than synthetic drugs.

The energy levels for monoterpenes shown in the  $\Delta G$  table gave an opinion about the structure-activity relationship. It is not sufficient for inhibitor candidates possessing side chains containing one ring and hydroxyl groups to be able to show anthelmintic effectiveness with a large spectrum. The position of the hydroxyl group on the monocyclic

structure did not cause a serious change in binding energy. This case can be seen in the isomers thymol and carvacrol or  $\gamma$ -terpinen and  $\alpha$ -terpinen.  $\Delta G$  values of these isomer duals were found very near to each other. AsFR, CPT 2, and Hc $\beta$ -tubulin have unnecessary large binding cavities to bind monoterpenes in Table 1. In the inhibition of these proteins, the molecules should be preferred to possess both at least a bicyclic or tetracyclic core structure and branched side groups containing oxygen or sulfur atoms. According to the values in Table 1, a monoterpene scaffold is more suitable for enzymes or receptors containing smaller binding cavities. These findings showed that monoterpene scaffold had a different action mechanism than benzimidazoles or macrocyclic lactones.

Charantadiol-A, momordicin I and II, kuguacin-J, karavilagenin-D, and cucurbitacin-B are compounds found in *M. charantia*. Two compounds, cucurbitacin-B and momordicin II, demonstrated the highest CPT 2 enzyme inhibition scores in this study, making them the most potent ligands as anthelmintics. Momordicin II is the second ligand possessing the best inhibition score, with a 72,69 pM  $K_i$  value in the fifty herbal ligands searched in this study (Fig. 3). Thanks to its exceptional inhibition ability, Momordicin II showed better results than the five synthetic drugs (IVC, MBZ, ABZ, piperazine, and PZQ) identified *in silico*. For instance, IVC showed very successful inhibition ability to the CPT 2 enzyme with a 290 pM value, but Momordicin II and cucurbitacin-B exhibited even better binding affinity.

Another important result is that the usage of the *M. charantia* extracts in oil-based solvents can be very effective as a herbal drug because these six herbal ligands were found to

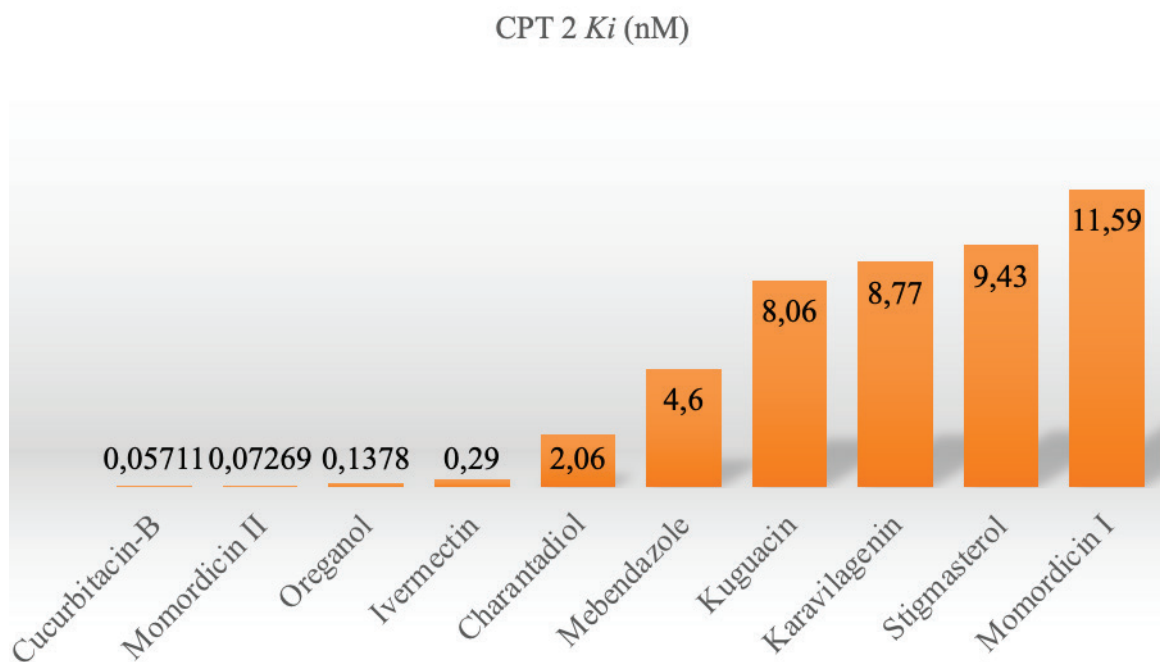


**Figure 3.** The first ten molecules possessing the best  $K_i$  values for CPT 2 enzyme.

have very favourable inhibition constants. Four of these six ligands (charantadiol-A, momordicin II, karavilagenin-D, and cucurbitacin-B) showed an inhibition effect on the AsFR enzyme at nanomolar levels. This desired result showed that these triterpenoids in *M. charantia* could be evaluated in developing dual-acting drugs. These results provided the necessary information for the development of a novel and more effective anthelmintic drug than the drugs on the market. According to the results of this study, in the future, some of the most effective anthelmintics will be cucurbitacins-based. For the first time in this study, it was reached the necessary *in silico* scientific data for this foresight.

Diosmetin, apigenin, oreganol, eriodictyol, luteolin, and crysoeriol in *O. vulgare* infusion; arteannuin-B, isofraxidin, umckalin, scopoletin in *A. annua* L. were found

inhibition ability with very good  $K_i$  values against three proteins which were docked. Therefore, these molecules are available to drug candidates in the development of large-spectrum anthelmintics. It approves the anthelmintic potential of these two plants because these molecules are in *O. vulgare* subsp. *hirtum* and *A. annua* L.

#### ADME Evaluation

In this study, the ligands possessing the best binding affinity among the fifty herbal ligands investigated in terms of AsFR, CPT 2 and Hc $\beta$ -tubulin inhibition in docking experiments were evaluated by the SwissADME web server to investigate their pharmacokinetics. The radar plot of oreganol shows that the solubility, unsaturation, flexibility, lipophilicity and size of the molecule are within

**Table 2.** ADME properties of the best ligands in terms of B-tubulin, CPT2 and AsFR inhibition

	Oreganol	Arteannuin-B	Apigenin	Cucurbitacin-B	Charantadiol-A	Momordicin II
Radar Plot						
Molecular weight	438,38 g/mol	248,32 g/mol	270,24 g/mol	558,70 g/mol	454,68 g/mol	634,84 g/mol
TPSA	186,3 Å <sup>2</sup>	38,83 Å <sup>2</sup>	90,90 Å <sup>2</sup>	138,2 Å <sup>2</sup>	49,69 Å <sup>2</sup>	156,91 Å <sup>2</sup>
Pharmacokinetics						
GI absorption	Low	High	High	Low	High	Low
BBB permeant	No	Yes	No	No	No	No
P-gp substrate	No	No	No	Yes	Yes	Yes
Log $K_p$ (skin permeation)	-8,95 cm/s	-5,98 cm/s	-5,80 cm/s	-7,83 cm/s	-3,85 cm/s	-7,57 cm/s
CYP1A2,	No	No	Yes	No	No	No
CYP2C19,	No	No	No	No	No	No
CYP2C9,	No	No	No	No	Yes	No
CYP2D6,	No	No	Yes	No	No	No
CYP3A4 inhibitor	No	No	Yes	Yes	No	Yes
Druglikeness						
Lipinski	No, 2 violations; NorO>10, NHorOH>5	Yes	Yes	Yes 1 violation: MW>500	Yes 1 violation: MLOGP>4,15	No, 2 violations: MW>500, NHorOH>5
Ghose	No	Yes	Yes	No	No	No
Veber	No	Yes	Yes	Yes	Yes	No
Egan	No	Yes	Yes	No	No	No
Muegge	No	Yes	Yes	Yes	No	No
Bioavailability Score	0.17	0.55	0.55	0.55	0.55	0.17

GI: Gastrointestinal; BBB: Blood-brain barrier; P-gp: P-glycoprotein; TPSA: Topological polar surface area; MW: Molecular weight; FLEX: Flexibility; LIPO: Lipophilicity; SIZE: Size; POLAR: Polarity; INSOLU: Insolubility; INSATU: Insaturation.

reasonable limits. Oreganol has poor GI absorption and cannot penetrate the blood-brain barrier. It was predicted that it would not inhibit any of the cytochrome enzymes in Table 2 and would not be a p-gp substrate. These features show that oreganol will not cause any problems in terms of side effects. Although further studies are needed to investigate its side effects, in this *in silico* study, oreganol stood out as an ideal ligand that could cause minimal side effects in ADME results. The possible inhibition mechanism of this molecule, which may be effective in killing helminths in the GI tract, seems to occur through simultaneous inhibition of the beta-tubulin protein and FR enzyme in the nematode.

Among these molecules, oreganol is the molecule that can penetrate through the skin the fastest, with a value of  $-8.95$  cm/s. Momordisin II, a larger molecule than oreganol, can penetrate through the skin quickly, although not as quickly as oreganol. Although it has fewer hydrogen bond acceptors and donor atoms than oreganol, momordicin II also cannot penetrate the blood-brain barrier and has poor GI absorption. Unlike oreganol, momordicin II may also act as a P-gp substrate, thus potentially slowing the efflux pump of the drug. Charantadiol-A is close to oreganol in terms of molecular weight and size, but unlike it, the number of hydrogen bond acceptors and donors is much less. Thus it fits three of Lipinski's rules. TPSA value was found to be  $49.69$  Å<sup>2</sup>. As seen in the radar graphic, the molecule is quite lipophilic and its water solubility is very low. Charantadiol-A is a molecule with high GI absorption. This triterpenoid molecule, which may be effective in eliminating helminths found outside the GI tract, can be used by dissolving it in oil-based solvents.

As seen in Table 2, cucurbitacin-B is a triterpenoid with a molecular weight of  $558.7$  g/mol, which has poor GI absorption and can through the skin at a speed of  $-7.83$  cm/s. Applying *M. charantia* fruits soaked in olive oil to the skin as a folk treatment is compatible with these ADME results, and applying this compound through the skin is a correct form of application. Although it is not shown in the table, the ILOGP value of cucurbitacin-B was found to be  $3.77$ , and since it is less than  $5$ , this molecule has a lipophilic character, therefore it can easily penetrate through the cell membrane and be used by dissolving in oil.

Apigenin, the most potent herbal inhibitor against Hc $\beta$ -tubulin with a  $K_i$  value of  $13.24$  nM, fully complies with Lipinski's and Egan, Muegge, Veber and Ghose's rules. It cannot penetrate the blood-brain barrier but has high GI absorption.

Among the ligands whose ADME properties were evaluated, the only molecule that had the most favorable results was suitable for oral administration, and could penetrate the blood-brain barrier was arteannuin-B. This small molecule can inhibit Hc $\beta$ -tubulin with a very low  $K_i$  value at  $14.95$  nM. Arteannuin-B has a high GI absorption and can be absorbed through the skin moderately. It fits all the rules of Lipinski, Ghose, Egan, Veber and Muegge, and its chemical properties fall within the reasonable limits of oral

intake. This molecule is moderately apolar and lipid soluble. It does not inhibit any important cytochrome enzymes in the liver listed in Table 2. It has a highly desirable polar surface area with a TPSA value of  $38.83$  Å<sup>2</sup>. All these positive features have shown that arteannuin-B is a very important drug candidate that can be taken orally and can even be used in the elimination of helminths settled in the nervous system. In a situation where resistance is developing against benzimidazoles, especially MBZ and ABZ, which have been donated at record levels and used by hundreds of millions of people for many years, arteannuin-B has emerged as a very valuable herbal ligand and a potential drug that can replace benzimidazoles with its tremendous ADME properties and highly successful inhibition ability.

### Best Ligands and Their Interactions

Among the herbal ligands in this study, in addition to oreganol, are among the components that can be found in the *O. vulgare* subsp. *hirtum*, cucurbitacin-B, momordicin II and charantadiol-A contained in *M. charantia* were examined in detail regarding their possible interactions with target proteins and the results were evaluated. When the chemical interactions and biological activity shown are evaluated together, some new mechanisms and pathways that can be used to discover new drug candidates to be developed through CADD can be predicted. In this respect, carefully examining possible interactions and interpreting new data on structure-activity will provide important information to researchers working on anthelmintic herbal ligands.

### Evaluation of Interactions of Oreganol

Oreganol [3-hydroxy-4-[(2*S*,3*R*,4*S*,5*S*,6*R*)-3,4,5-trihydroxy-6-(hydroxymethyl) oxan-2-yl]oxyphenyl] methyl 3,4-dihydroxybenzoate] is a glycoside (Computed by LexiChem 2.6.6, PubChem, 2019). Its 2D molecular structure is given in Figure 4.

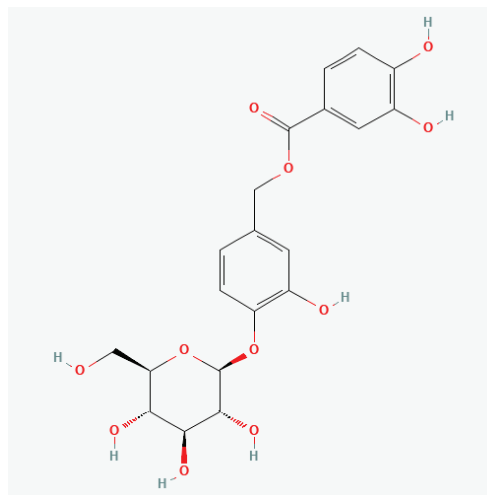
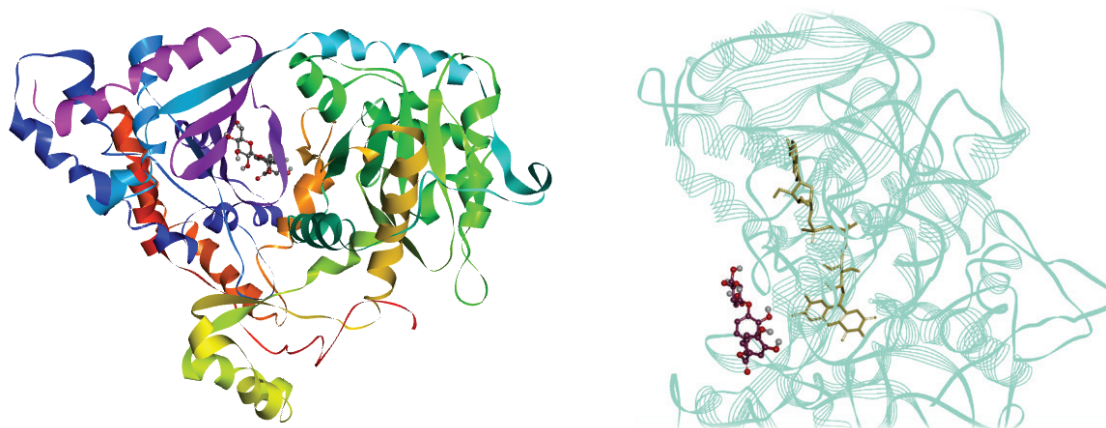
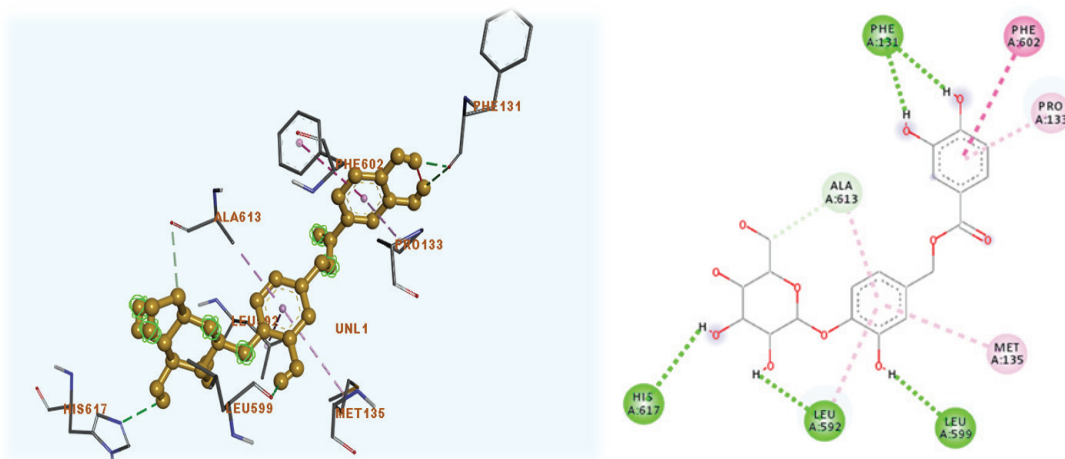


Figure 4. Oreganol 2D representation (from PubChem).



**Figure 5.** Positioning of oreganol in target enzymes. A) in CPT 2 (pdb ID: 2H4T), B) in AsFR (pdb ID: 4YSX). Oreganol was represented with a ball and stick, FAD cofactor with a yellow stick, and protein with blue ribbon models.



**Figure 6.** Possible chemical interactions of oreganol in the rat CPT 2 (pdb ID: 2H4T) enzyme and the residues it interacts with. A) Interactions are shown with dashed lines and oreganol orange ball-and-stick model B) 2D representation.

The active site of the CPT 2 enzyme is wider than the active site of  $\beta$ -tubulin, and the positioning of oreganol in the rat CPT 2 enzyme is shown in Figure 5. Since the coordinates of the region where the ligand binds were determined previously, the same coordinates were used in the docking simulations in this study. Therefore, the placement of the ligand in the active site is compatible with the literature [7]. As shown in Figure 5A, oreganol settled into the space created by the  $\beta$ -conformation and loop structure. In Figure 6, the two hydrogen bonds made by oreganol with PHE131 are noteworthy. The central ring of oreganol was sandwiched between ALA613 and MET135. The dihydroxyphenyl residue also formed an aromatic sandwich between PHE602 and PRO133. In Figure 5B, oreganol was located in front of the FAD cofactor in AsFR enzyme. Four hydrogen bonds (possessing 2,18 Å distance with ALA83, 2,09 Å with THR81, 2,13 Å with THR 248, and 2,76 Å with

THR 247) were predicted between oregano and AsFR (PDB ID: 4YSX) (Fig. 7 B).

According to Figure 6 B, four residues in the CPT 2 active site formed hydrogen bonds with the hydrogen atoms in the hydroxyl groups of oreganol. These residues are PHE131, HIS617, LEU592 and LEU599. Additionally, PRO133 made a strong  $\pi$ -alkyl interaction with the dihydroxyphenyl ring of oreganol in close proximity. MET135 also formed another  $\pi$ -alkyl bond at a longer distance from the central ring. While the PHE602 residue interacted with the dihydroxyphenyl group of oreganol in a  $\pi$ - $\pi$  T-shaped interaction, the ALA613 residue interacted with the central ring of the ligand with pi-alkyl interaction.

As a significant result, five hydrogen bonds were seen in the interactions of oreganol with *H. contortus*  $\beta$ -tubulin. One of them was performed between the hydroxyl group of

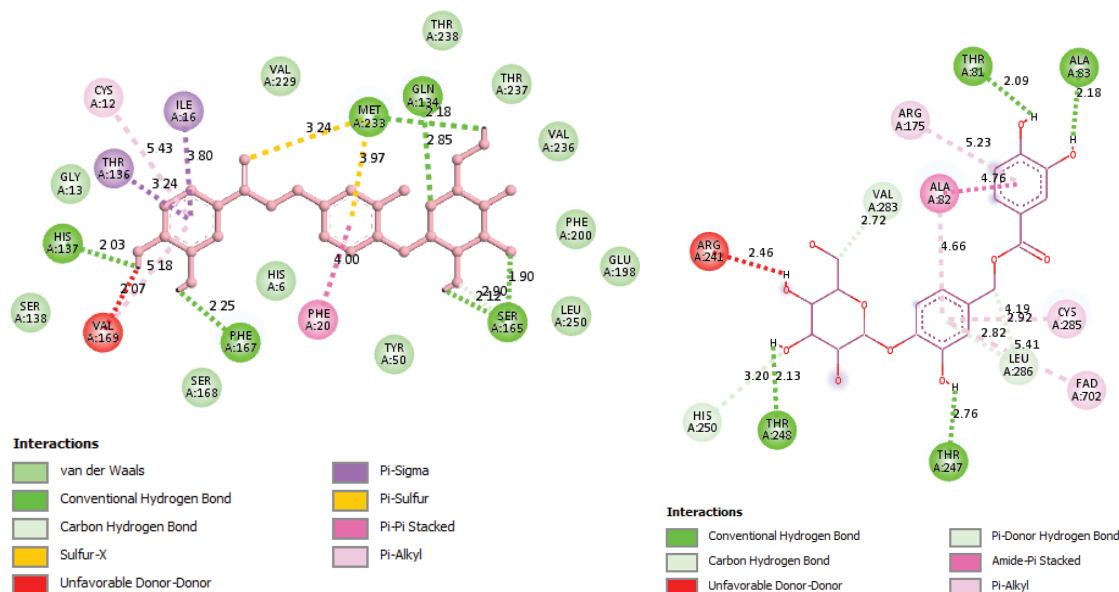


Figure 7. 2D representation of Oreganol A) in *H. contortus*  $\beta$ -tubulin B) in AsFR enzyme.

oreganol and PHE167 residue being sensitive to mutation. Probable interactions are shown in Figure 7 A.

#### Possible Interactions of Momordicin II in Rat CPT 2

A dense interaction network can be seen in Figure 8, where the possible interactions of momordicin II within the rat CPT 2 enzyme (pdb ID: 2FW3) are shown. Although the majority of these interactions in Figure 8 were van der Waals attraction forces, there were four polar and one nonpolar residue where hydrogen bond formation was predicted. These hydrogen bonds were formed through

residues TYR614, THR591, LEU592, SER590 and ASN130. Apart from this, HIS372 made both  $\pi$ -sigma bonds and  $\pi$ -alkyl interactions. Other residues responsible for  $\pi$ -alkyl interactions were PRO133, PHE370, PHE602, TYR486, VAL605 and PHE131. The residues that made van der Waals interactions were SER588, SER488, ALA613, ILE612, GLU601, ALA615, ASN593, VAL587, MET135, GLY377, ASP376, TRP116, TYR120, and THR499.

In Figure 8, although there is a repulsion force between SER590, which is a polar residue, and the oxygen atom of momordicin II, and another repulsion force is predicted to

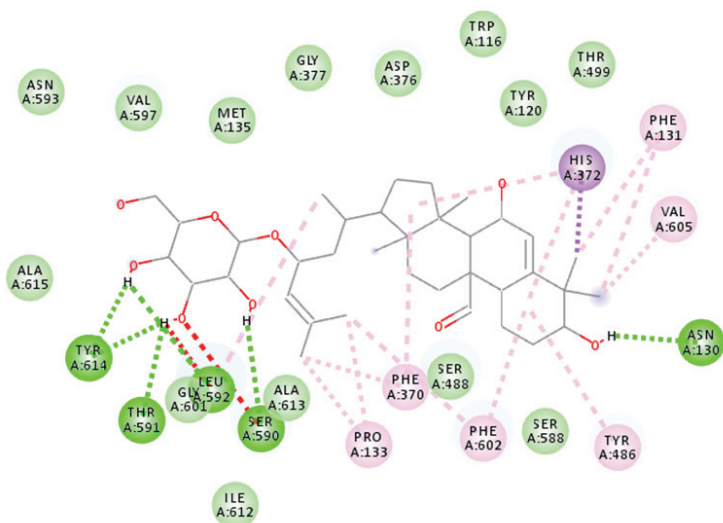
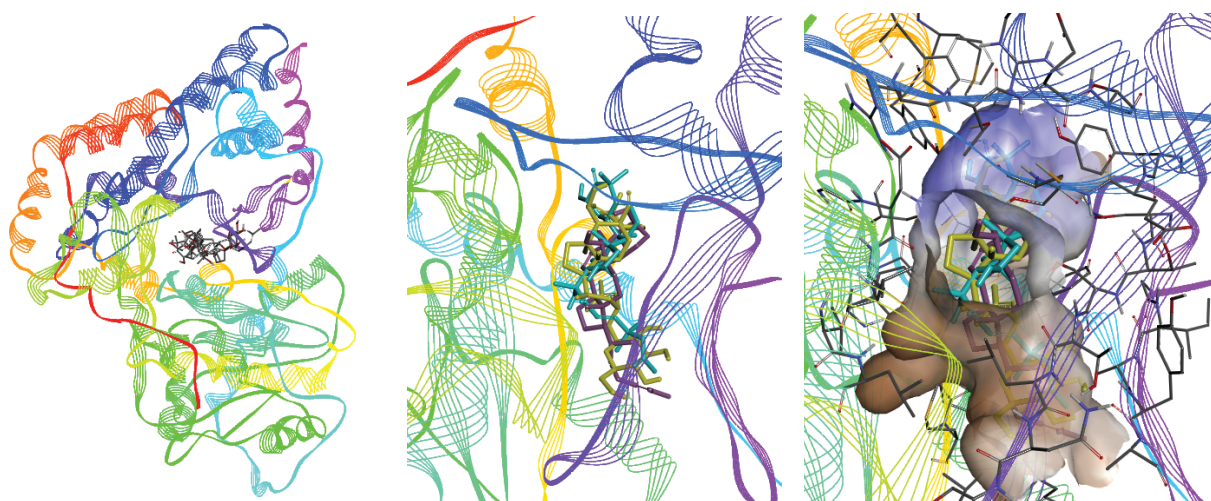


Figure 8. 2D representation of momordicin II and rat CPT 2 (pdb ID: 2FW3) interactions.



**Figure 9.** Positioning of momordicin II (yellow), charantadiol-A (purple) and cucurbitacin-B (blue) in 2FW3. The protein is shown in rainbow colors. The hydrophobicity of the residues in the region surrounding the ligands (rightmost image), the blue regions represent the hydrophilic parts and the brown regions represent the hydrophobic parts.

occur between the hydrogen atom of LEU592, a nonpolar residue, and the hydrogen atom bonded to the hydroxyl group of momordicin II, the formation of numerous hydrogen bonds between the part carrying the hydroxyl group of the ligand and the surrounding residues caused the free binding energy to decrease.

#### Possible Locations of Momordicin II, Charantadiol-A and Cucurbitacin-B In Rat CPT 2 (PDB ID: 2FW3)

Both charantadiol-A and cucurbitacin-B are similar to momordicin II in terms of molecular size, and these three molecules are among the top five molecules with the best

binding energies for the rat CPT 2 enzyme (see Figure 3). In addition, it can be seen in Figure 9 that there is a similarity in terms of the structures and torsions of the molecules.

In the design of a pharmacophore, it is significant to know the aromatic surface of the binding cavity. According to these surface properties, chemical groups can be substituted for the scaffold. In Figure 10, the aromatic surface was shown in the CPT 2 enzyme (PDB ID: 2FW3) when it docked with cucurbitans.

Nonpolar residues such as valinyl, glycyl, alaninyl and leucinyl enable the formation of a more hydrophobic binding surface (Fig. 10).

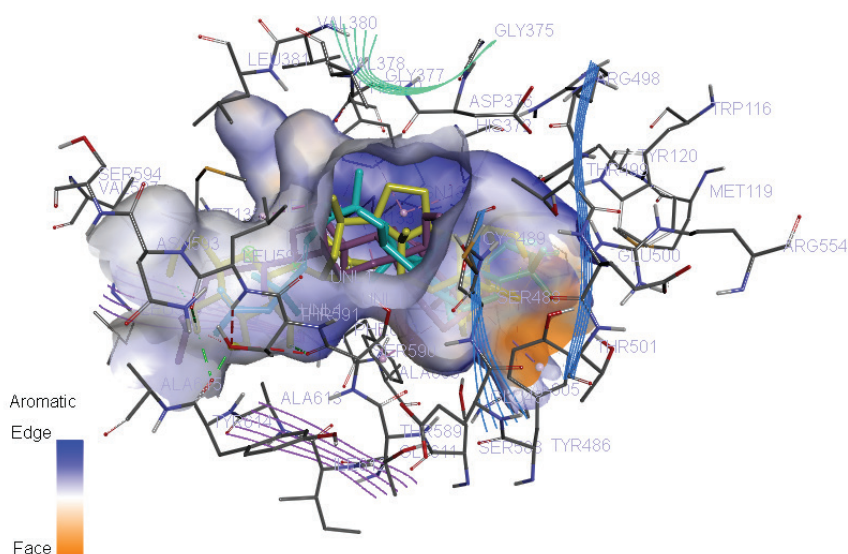


**Figure 10.** Surrounding the ligands, the blue regions represent the aromatic ends and the red regions represent the non-aromatic parts.

### Evaluation of Interactions of Cucurbitacin-B and CPT 2 Enzyme (PDB ID: 2H4T)

In this study, the herbal ligand that can inhibit the CPT 2 enzyme with the most appropriate free energy of binding is cucurbitacin-B and its  $K_i$  value was 57.11 pM and  $\Delta G$  value was -13.98 kcal/mol. The results of cucurbitacin-B were followed by momordicin II, another cucurbitan class molecule, and with its value of 72.69 pM, it is also a very successful inhibitor candidate. The locations of momordicin II and cucurbitacin-B in the CPT 2 enzyme (pdb code: 2FW3) were examined by superimposing them for easier comparison (Fig. 9). The interactions of cucurbitacin-B in 2H4T are explained in detail in the figures below.

While cucurbitacin-B was located in the cavity in the binding site of the CPT 2 enzyme, it was surrounded by  $\alpha$ -helices on one side and  $\beta$ -sheet structures on the other. Since cucurbitacin-B is a large molecule in the triterpenoid class, it could only fit into this cavity by standing parallel to the parallel  $\beta$ -sheets surrounding it. As seen in Figure 11, the long side chain attached to the core structure of the ligand stood very close to the two-loop structure of the protein and managed to locate the cavity by approaching the cavity formed by the  $\beta$ -sheet structure, shown in blue, which takes the shape of a half-moon.

MET 135, GLY 600, SER 590, TYR 614 and PRO 133 are the residues shown in yellow in Figure 11 and are located on the secondary structures interacting with cucurbitacin-B. It is shown in Figure 11 that the structures that cucurbitacin-B interacts with are its two-loop structure and some small regions on  $\beta$ -sheets and that it does not interact with  $\alpha$ -helices but can only interact with a small part of an  $\alpha$ -helix.

The long side chain of cucurbitacin-B interacted with three different  $\beta$ -sheets, and Figure 11 shows that the residues with which it interacts were ALA 613, GLY 601, PHE 134, LEU 592 and PHE 602. The steroid ring of the ligand is attracted by ASN 593 and SER 488, which are predicted to be located on the loop structures of the protein. It is estimated that SER 488 was the only residue among these residues that attracted the ligand from the opposite direction, and the fact that the steroid ring structure of the ligand was folded in an L shape made it easier for it to be attracted by many residues on the other side.

Cucurbitacin-B did not use the ring structures in the center in aromatic interactions, and the two phenylalanine residues formed reversible bonds only with the polar side chain of the ligand (Fig. 12). The most important of these are the 2.2 Å long hydrogen bond formed between PHE 134 and the oxygen atom of the ligand and the 2.31 Å long hydrogen bond formed between the same oxygen and GLY 601. Other important hydrogen bonds were seen between the lanostan ring and ASN 593, one of which is 1.78 Å long and formed with the oxygen atom of the ligand, and the other is the 2.27 Å long hydrogen bond formed with the hydroxyl group of the ligand (Fig. 12). Another hydrogen bond, which was shown to be quite strong, occurred between the hydroxyl group attached to the pentane ring of cucurbitacin-B and SER 488 at a distance of 1.95 Å. As shown in the figure, LEU 592 and PHE 602 made  $\pi$ -alkyl interactions with the ligand, and ALA 613 made two  $\pi$ -alkyl interactions.

The residues which cucurbitacin-B interacts with van der Waals in the CPT 2 enzyme are HIS 372, PHE 370, SER 490, GLY600, MET 135, SER 590, THR 591, LEU 381 and VAL 378, shown as light green spheres.

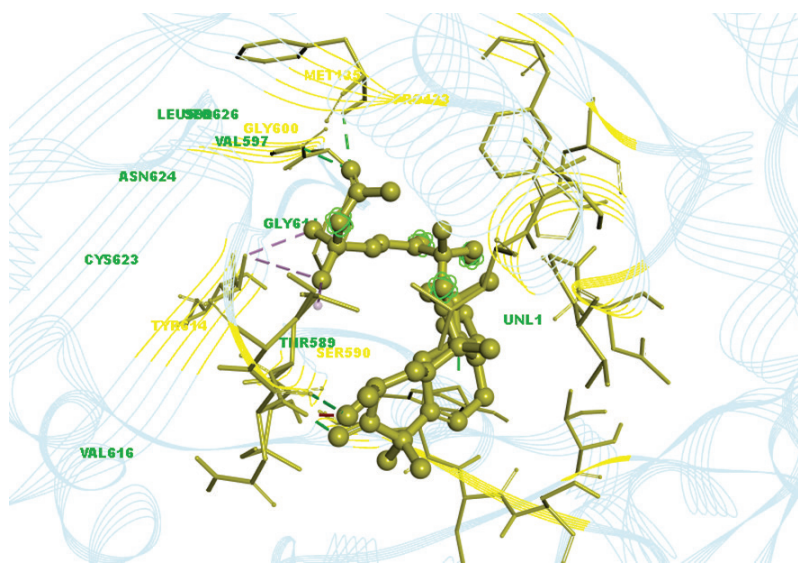


**Figure 11.** Cucurbitacin-B, in the CPT 2 enzyme binding region, the regions and amino acids with which it interacts closely are written with yellow, van der Waals interactions with green.

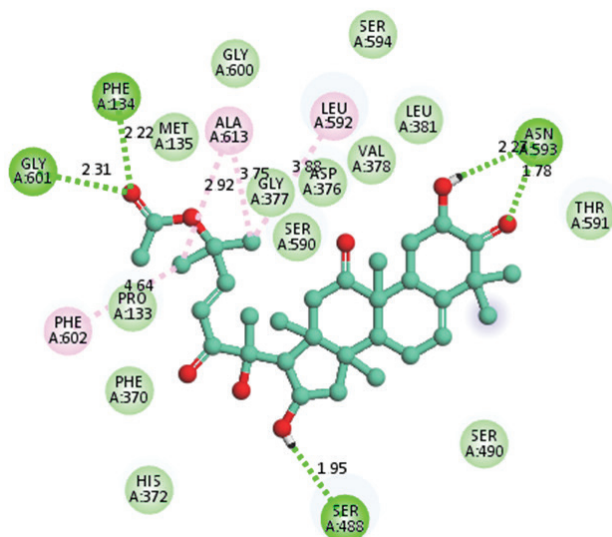


**Figure 12.** 2D representation of the possible interaction network of cucurbitacin-B and CPT 2 enzyme. Cucurbitacin-B is represented in the center with a ball-and-stick model, with carbon atoms in green, oxygens in red, and hydrogens in white.  $\pi$ -alkyl interactions within the protein are shown as pink dashed lines and hydrogen bonds as green dashed lines.

The values shown for the inhibition of CPT 2 enzyme (2FW3) prove that cucurbitacin-B, momordicin II, oreganol and charantadiol-A can show an anthelmintic effect by affecting lipid metabolism. While reversible inhibition of CPT 2 enzyme does not cause any significant side effects, metabolites produced in case of short-term inhibition lead to the death of some helminth species [7].

The results in Figure 13 show the using of correct points in selecting the grid box center in the docking procedure greatly affects the results. The coordinates of the selected center for 2H4T were taken from Taylor et al. [7]. For 2FW3, the center region of the protein was taken as the center. Although a grid box of 60×60×60 was created for both of them, the automatic determination of the center for 2FW3 caused changes in the  $\Delta G$  values.

It is important to understand the effect pathway of cucurbitacin-B working as an anthelmintic compound. CPT 2 inhibition results from the increasing level of CPT 2 substrates, and this condition causes the death of helminths (Fig. 14).

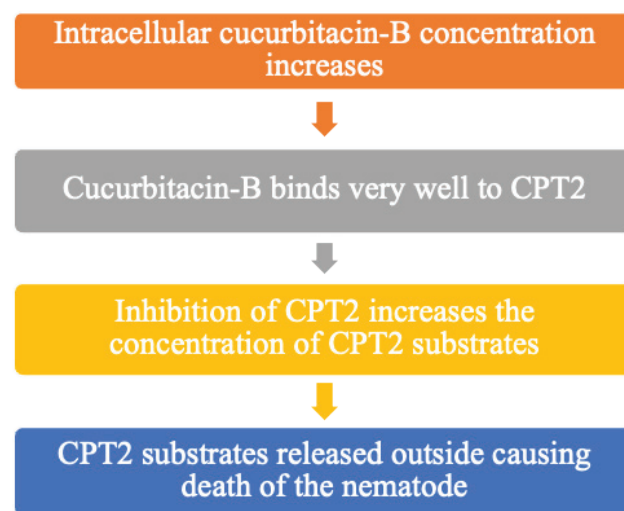


**Figure 14.** Flow chart of the CPT2-related mechanism of action of cucurbitacin-B.

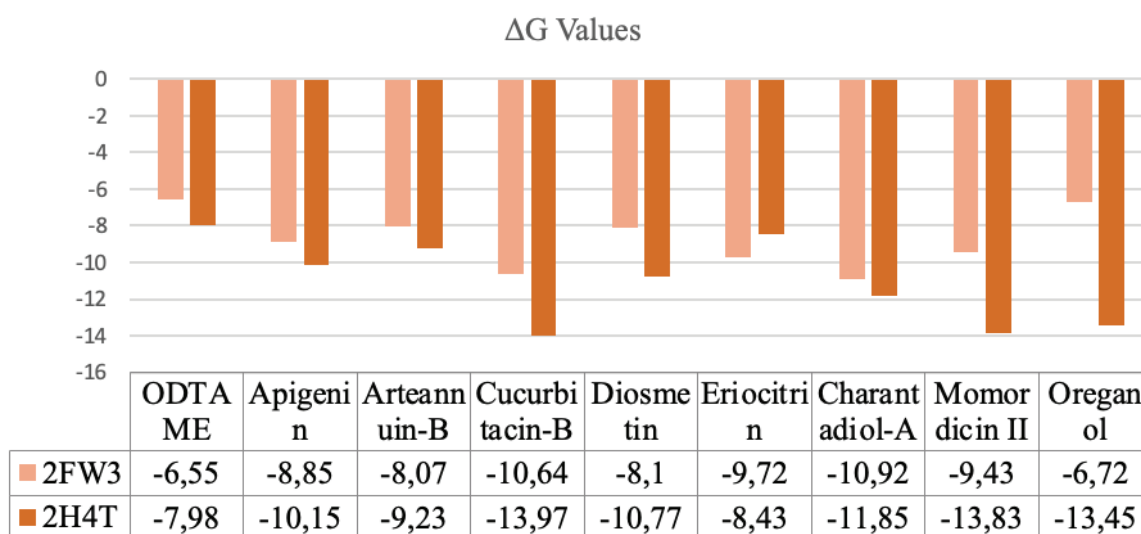


**Figure 13.** Comparison of the  $\Delta G$  values found in the dockings of nine ligands with 2FW3 and 2H4T (CPT 2 enzyme).

In some important studies, active compounds in the plants were searched via *in silico* methods, and the predictions were presented on the activity of herbal ligands. The theoretical structure of Hc $\beta$ -tubulin used in this current study has been tried in molecular docking experiments to evaluate the anthelmintic effects of some derivative molecules [20]. Hc $\beta$ -tubulin is an important antinematodal target, but there is no crystallographic structure of Hc $\beta$ -tubulin in any database, and it is the first time the theoretical structure in this study shows the anthelmintic properties of herbal secondary metabolites. In another study, compounds such as ellagic acid, quercetin, isoquercetin, and caffeic acid in *Achyrocline satureioides* were isolated. Then caffeic acid was searched *in silico* and *in vitro* regarding antioxidant and toxicological activities. As a result, the prediction of *in silico* toxicity of quercetin, isoquercetin, and caffeic acid showed a low toxic risk [21]. While it was being researched *in vivo* anthelmintic effect of *Cordia dichotoma* (Forst.) root extract, the compounds that had been shown to have existed in this plant were searched *in silico* [22]. Like in this current study, it was predicted *in silico* which compounds are related to the biological activity of the extract. They also carried out docking experiments with the target protein by selecting the components according to the results of the literature screening without purifying them. In this way, they predicted which component caused the biological activity of the extracts. However, in the literature, there are not any dual-acting herbal compounds that can inhibit the target enzymes at pM levels *in silico*.

Among the bioactive compounds contained in the plants evaluated in this current study, those found in the highest amounts as specific to the plant were determined according to the results of previously conducted spectroscopy and chromatography analyses [23–25]. The results of this study can be used to reduce workload and cost. This data can be evaluated before purifying these components one by one in future studies and investigating their anthelmintic effects via *in vivo* and *in vitro* studies. With the Hybrid NAR-RBFs Networks simulation, the spread of helminthic diseases in the world can also be investigated [2]. Thus, an important study will be carried out to control diseases affecting millions of people.

Essential oil and water extract of *O. vulgare* were shown to have an antiproliferative effect on some cancer cells *in vitro*. Carvacrol, being the most abundant compound, was shown to a 90,42% range in the essential oil of *O. vulgare*. In comparison to essential oil and extract, it was found that essential oil has a more antiproliferative effect than water extract. However, the cytotoxicity of the extract was more than that of the essential oil [26]. It should be investigated that this cytotoxic effect of the water extract is related to which secondary metabolites of oregano. These secondary metabolites can show a similar cytotoxic effect on helminth cells.

It was discovered that the *Origanum* extract (10 mg/ml) has ovicidal activity on egg hatching of *Haemonchus*

*contortus*, depending on the dose [27]. The antiparasitic effect of oregano oil was also previously shown [28]. However, in this study, the docking results of carvacrol and thymol, the main components of oregano oil, did not indicate a significant anthelmintic property. This result was attributed to the small number of interactions of the molecules within the target proteins. The oreganol found in oregano infusion was shown for the first time to have a very significant anthelmintic potential. Oregano oil is a highly irritating liquid and is unpleasant to take orally. Oregano tea is both delicious and beneficial to health [29].

Artemisinin is both an anthelmintic agent on *H. contortus* [30] and has been used for antimalarial purposes for years, and is the reason why the *A. annua* L., from which it is obtained, is planted in large areas. However, arteannuin-B has not been studied as much as artemisinin, and the great potential of this molecule is ignored. In this study, while it was shown in ADME research that arteannuin-B is suitable for oral administration, it was also shown through molecular docking that it has the potential to inhibit B-tubulin and AsFR enzymes. Arteannuin-B is a drug candidate that deserves more detailed research.

The antinematodal effect of bitter melon on swine nematode was shown in a previous study. 70% ethanolic extract of *Momordica charantia* L. folium showed the lethal effect on *Ascaris suum* at the 88% range [31]. In this study, the molecular mechanism of secondary metabolites that could cause this effect was investigated.

Most helminth species feed and survive by absorbing glucose via the cells outside their bodies. Since momordicin I and II, two active compounds found in bitter melon can inhibit glucose absorption [32], these two active compounds are good candidates to show the anthelmintic effect. This is the first study showing the antihelmintic effect of cucurbitacin-B and momordicin II that can inhibit antinematodal targets CPT2 and AsFR with favorable *Ki* values at very low levels.

One of the most important results from this study is that a branched side chain attached to cyclopentane in the steroid ring directly affects the affinity to the CPT 2 binding site. In addition, cucurbitacin-B, momordicin II, charantadiol-A, stigmaterol and friedelin, which have a large core with the union of at least four rings, require a slightly larger cavity to displace in the protein, which prevents them from being positioned in tubulin. This result provided new data that can be evaluated in the discovery of alternative drugs with fewer side effects than ABZ. Docking analyses of these molecules support this. These ingredients are promising in eliminating nematode species found in the gastrointestinal system (GIS), especially those that disrupt the cognitive and physical development of children. As a result of the screening performed with the SwissADME web server, the GI absorption of these compounds was found low. However, these properties will have a positive effect on increasing the inhibition against helminths in the GI system. Thus, the concentration of these molecules in the GIS will not

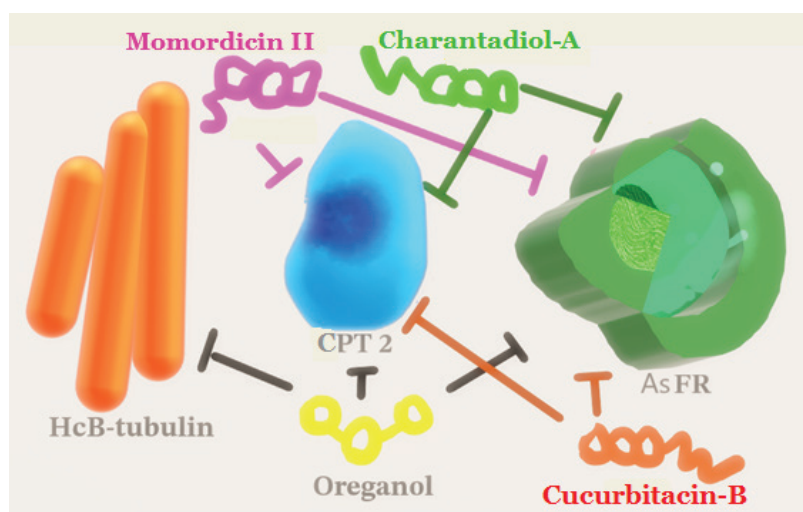


**Figure 15.** Inhibition diagram of most potent herbal ligands.

decrease easily, and helminths will be exposed to these molecules more intensely. Normally, these triterpenoid molecules are insoluble in water, and these components can be taken orally with oil-based solvents. Since the monoterpenes contained in Oregano essential oil can easily pass through the cell membrane and penetrate the skin, they can be evaluated in developing drugs that can be applied as ointments against parasites that form nodules on the skin. In this respect, it is a rational approach to investigate GABA receptors specific to parasites such as Dracunculiasis as primary targets in developing monoterpene-based inhibitors.

Some derivative molecules can show more effectiveness on the same target enzyme if the substituted groups are changed or added. Some eriocitrin derivatives were found to be more effective than eriocitrin in the CPT 2 inhibition, and this result signed a more potential inhibition ability for a derivative molecule possessing a natural glycoside scaffold [33]. Arteannuin-B is a potential anthelmintic drug scaffold, according to the current study in terms of ADME results and inhibition constants for B-tubulin inhibition. Therefore, arteannuin-B can be chosen for the rational *in silico* drug design of novel derivative molecules in the case of benzimidazole resistance. Corporations have been donating millions of tablets benzimidazoles each year. Therefore, resistance development can be seen in the near future.

The docking simulations of this study revealed that the most rational drug combinations might be oreganol + cucurbitacin (charantadiol-A, momordicin II, or cucurbitacin-B). This combination also seems suitable as a broad-spectrum drug candidate because oreganol inhibits Hc $\beta$ -tubulin, while cucurbitacin ligands can inhibit AsFR and CPT 2 at low concentrations. At the same time, oreganol is triple-acting inhibitor and these cucurbitacins are dual-acting inhibitors (Fig. 15). Cucurbitacin-B, charantadiol-A, and momordicin II inhibited CPT 2 and AsFR enzymes at nanomolar inhibition constants (5,31 nM, 16,6 nM, and 40,78 nM for AsFR;

0,0571 nM, 2,06 nM, and 0,072 nM for CPT 2 enzyme, respectively). As oreganol inhibited all of these enzymes at low  $K_i$  values ( $K_i = 24,32$  nM for Hc $\beta$ -tubulin, 1,9 nM for AsFR, and 0,137 nM for CPT 2 enzymes). In the literature, there is limited information about oreganol and there is no data about the anthelmintic property of this compound. It is the first study to show the anthelmintic effect of oreganol *in silico*.

These results will guide researchers who aim to design or synthesize drugs for the treatment of various helminthic diseases and thus positively affect the health of millions of people. This study provides new data regarding structure-activity and suggests a scaffold to replace Ivermectin from macrocyclic lactones. Ivermectin is a drug licensed only for use in animals, but since there is no alternative, it is used in humans to treat *O. volvulus* infection. Approximately 270.000 people are infected with this nematode, which causes blindness [1]. Therefore, there is an urgent need to discover new drugs for its treatment.

## CONCLUSION

According to the results of this study, cucurbitacin-B is an alternative drug candidate to Ivermectin.

It is also important for an anthelmintic drug candidate to have a broad spectrum to use fewer drug and to have easier access. Since oreganol has inhibitory properties for three different target proteins in this study, it has the potential to meet this desired broad-spectrum need.

Most importantly, when considered as a folk medicine, since oreganol is found in oregano infusion and cucurbitacins are found in the fleshy fruit and leaves of the bitter melon, it was estimated in this study with *in silico* calculations that oregano tea and bitter melon fruit would be useful in removing of parasitic worms in the body.

These molecular docking results show that herbal compounds could be broad-spectrum anthelmintic drugs with multi-inhibition properties. This is significant because it demonstrates that anthelmintics, often required, can be obtained from oregano and bitter melon. This study is the first to demonstrate the potential interactions of these compounds with target proteins. Oreganol was first shown as an anthelmintic secondary metabolites possessing triple-acting inhibition ability. Cucurbitans are worth researching with further *in vivo* studies for the treatment of *O. volvulus* infection. Oreganol, cucurbitacin-B, momordicin II and charantadiol-A should be isolated from plants and should be tried on target nematodal proteins and enzymes to observe the inhibition properties *in vitro*.

## ACKNOWLEDGEMENTS

We would like to dedicate this study to our esteemed professor, Prof. Dr. Metin Aktaş. His an epidemic disease in 83 is always alive.

We are very thankful to Özkılıç and Tüzün for their informational support and inspirational article: “*In silico* methods predict new blood-brain barrier permeable structure for the inhibition of kynurenine 3-monooxygenase.”

## AUTHORSHIP CONTRIBUTIONS

Authors equally contributed to this work.

## DATA AVAILABILITY STATEMENT

The authors confirm that the data that supports the findings of this study are available within the article. Raw data that support the finding of this study are available from the corresponding author, upon reasonable request.

## CONFLICT OF INTEREST

The author declared no potential conflicts of interest with respect to the research, authorship, and/or publication of this article.

## ETHICS

There are no ethical issues with the publication of this manuscript.

## STATEMENT ON THE USE OF ARTIFICIAL INTELLIGENCE

Artificial intelligence was not used in the preparation of the article.

## REFERENCES

- [1] World Health Organization. Parasitic Infections. Available at: <http://www.who.int/mediacentre/factsheets/fs366/en/>. Accessed on July 18, 2017.
- [2] Ahmad A, Farman M, Sultan M, Ahmad H, Askar S. Analysis of hybrid NAR-RBFs networks for complex non-linear Covid-19 model with fractional operators. *BMC Infect Dis* 2024;24:1–19. [CrossRef]
- [3] Yelekçi K, Büyüktürk B, Kayrak N. In silico identification of novel and selective monoamine oxidase B inhibitors. *J Neural Transm* 2013;120:853–858. [CrossRef]
- [4] Karaman D. Prediction on the Anthelmintic Effects of Some Herbal Ligands and Their Derivatives with In Silico Molecular Modelling Method [Doctoral thesis]. Bursa: Bursa Uludag University; 2022.
- [5] Daina A, Michielin O, Zoete V. SwissADME: a free web tool to evaluate pharmacokinetics, drug-likeness and medicinal chemistry friendliness of small molecules. *Sci Rep* 2017;7:42717. [CrossRef]
- [6] Kaplan RM. Drug resistance in nematodes of veterinary importance: a status report. *Trends Parasitol* 2004;20:477–481. [CrossRef]
- [7] Taylor CM, Wang Q, Rosa BA, Huang SCC, Powell K, Schedl T, et al. Discovery of anthelmintic drug targets and drugs using chokepoints in nematode metabolic pathways. *PLoS Pathog* 2013;9:1003505. [CrossRef]
- [8] Ceccarelli SM, Chomienne O, Gubler M, Arduini A. Carnitine palmitoyltransferase (CPT) modulators: a medicinal chemistry perspective on 35 years of research. *J Med Chem* 2011;54:3109–3152. [CrossRef]
- [9] Karaman D, Girişgin AO, Girişgin O. Is the Inevitable End or the Happy End? In Silico Anthelmintic Resistance Development Scenario, Arteannuin-B is in the Leading Role. In: *Proceedings of the International Asian Congress on Contemporary Sciences-V; 2021 Jun; Nakhchivan, Azerbaijan*. p. 741–749.
- [10] Centers for Disease Control and Prevention. Parasites - Onchocerciasis (also known as River Blindness). Available at: <https://www.cdc.gov/filarial-worms/treatment/onchocerciasis.html>. Accessed on December 6, 2024.
- [11] Dassault Systèmes. BIOVIA Discovery Studio Modeling Environment, Release 2020. San Diego: Dassault Systèmes; 2020.
- [12] Huey R, Morris GM, Olson AJ, Goodsell DS. A semiempirical free energy force field with charge-based desolvation. *J Comput Chem* 2007;28:1145–1152. [CrossRef]
- [13] Morris GM, Huey R, Lindstrom W, Sanner MF, Belew RK, Goodsell DS, et al. AutoDock4 and AutoDockTools4: Automated docking with selective receptor flexibility. *J Comput Chem* 2009;30:2785–2791. [CrossRef]
- [14] Inaoka DK, Shiba T, Sato D, Balogun EO, Sasaki T, Nagahama M, et al. Structural insights into the molecular design of flutolanil derivatives targeted for fumarate respiration of parasite mitochondria. *Int J Mol Sci* 2015;16:15287–15308. [CrossRef]

- [15] Robinson MW, McFerran N, Trudgett A, Houy L, Fairweather I. A possible model of benzimidazole binding to beta-tubulin disclosed by invoking an inter-domain movement. *J Mol Graph Model* 2004;23:275–284. [\[CrossRef\]](#)
- [16] Hsiao YS, Jogl G, Esser V, Tong L. Crystal structure of rat carnitine palmitoyltransferase II (CPT-II). *Biochem Biophys Res Commun* 2006;346:974–980. [\[CrossRef\]](#)
- [17] Rufer AC, Thoma R, Benz J, Stihle M, Gsell B, De Roo E, et al. The crystal structure of carnitine palmitoyltransferase 2 and implications for diabetes treatment. *Structure* 2006;14:713–723. [\[CrossRef\]](#)
- [18] Morris GM, Goodsell DS, Halliday RS, Huey R, Hart WE, Belew RK, et al. Automated docking using a Lamarckian genetic algorithm and an empirical binding free energy function. *J Comput Chem* 1998;19:1639–1662. [\[CrossRef\]](#)
- [19] Tyagi R, Maddirala AR, Elfawal M, Fischer C, Bulman CA, Rosa BA, et al. Small molecule inhibitors of metabolic enzymes repurposed as a new class of anthelmintics. *ACS Infect Dis* 2018;4:1130–1145. [\[CrossRef\]](#)
- [20] Satyendra RV, Vishnumurthy KA, Vagdevi HM, Rajesh KP, Manjunatha H, Shruthi A. Synthesis, in vitro antioxidant, anthelmintic and molecular docking studies of novel dichloro substituted benzoxazole-triazolo-thione derivatives. *Eur J Med Chem* 2011;46:3078–3084. [\[CrossRef\]](#)
- [21] Salgueiro AC, Folmer V, da Rosa HS, Costa MT, Boligon AA, Paula F, et al. In vitro and in silico antioxidant and toxicological activities of *Achyrocline satureioides*. *J Ethnopharmacol* 2016;194:6–14. [\[CrossRef\]](#)
- [22] Jamkhande PG, Barde SR. Evaluation of anthelmintic activity and in silico PASS assisted prediction of *Cordia dichotoma* (Forst.) root extract. *Anc Sci Life* 2014;34:39–43. [\[CrossRef\]](#)
- [23] Özcan MM, Pedro LG, Al-Juhaimi F, Endes Z, Erol AS, Duman E, et al. Constituents of the essential oil of *Origanum vulgare* subsp. *hirtum* growing wild in Turkey. *J Essent Oil Bear Plants* 2012;15:572–576. [\[CrossRef\]](#)
- [24] Li W, Lin Z, Yang C, Wang Y, Qiao Y. Study on the chemical constituents of *Momordica charantia* L. leaves and method for their quantitative determination. *Biomed Res* 2015;26:415–419.
- [25] Abu-Shandi K, Al-Rawashdeh A, Al-Mazaideh G, Abu-Nameh E, Al-Amro A, Al-Soufi H, et al. A novel strategy for the identification of the medicinal natural products in *Rubus fruticosus* plant by using GC/MS technique: A study on leaves, stems and roots of the plant. *Adv Anal Chem* 2015;5:31–41.
- [26] Erenler R, Çarlık ÜE, Aydın A. Antiproliferative activity and cytotoxic effect of essential oil and water extract from *Origanum vulgare* L. *Sigma J Eng Nat Sci* 2023;41:202–208. [\[CrossRef\]](#)
- [27] Castro LLD, Madrid IM, Aguiar CLG, Castro LM, Cleff MB, Berne MEA, et al. *Origanum vulgare* (Lamiaceae) ovicidal potential on gastrointestinal nematodes of cattle. *Cienc Anim Bras* 2013;14:508–513.
- [28] Pensel PE, Maggiore MA, Gende LB, Eguaras MJ, Denegri MG, Elissondo MC. Efficacy of essential oils of *Thymus vulgaris* and *Origanum vulgare* on *Echinococcus granulosus*. *Interdiscip Perspect Infect Dis* 2014;2014:693289. [\[CrossRef\]](#)
- [29] Treben M. *Health Through God's Pharmacy: Advice and Proven Cures with Medicinal Herbs*. 6th ed. Germany: Ennsthaler; 2007.
- [30] Cala AC, Ferreira JFS, Chagas ASC, Gonzalez JM, Rodrigues RAF, Foglio MA, et al. Anthelmintic activity of *Artemisia annua* L. extracts in vitro and the effect of an aqueous extract and artemisinin in sheep naturally infected with gastrointestinal nematodes. *Parasitol Res* 2014;113:2345–2353. [\[CrossRef\]](#)
- [31] Tjokropranoto R, Nathania M. Anthelmintic effect of ethanol extract of pare leaf (*Momordica charantia* L.) against female *Ascaris suum* worm in vitro. *J Medika Planta* 2011;1:33–39.
- [32] Liu H, Wang GC, Zhang MX, Ling B. The cytotoxicology of momordicins I and II on *Spodoptera litura* cultured cell line SL-1. *Pestic Biochem Physiol* 2015;122:110–118. [\[CrossRef\]](#)
- [33] Karaman D, Girişgin AO, Girişgin O. Eriocitrin derivatives and their anthelmintic potentials. *Sigma J Eng Nat Sci* 2024;42:875–884. [\[CrossRef\]](#)